

LIU, D., WANG, S., FAN, Y., FERNANDEZ, C. and BLAABJERG, F. 2024. A novel multi-factor fuzzy membership function - adaptive extended Kalman filter algorithm for the state of charge and energy joint estimation of electric-vehicle lithium-ion batteries. *Journal of energy storage* [online], 86(part A), article number 111222. Available from: <https://doi.org/10.1016/j.est.2024.111222>

A novel multi-factor fuzzy membership function - adaptive extended Kalman filter algorithm for the state of charge and energy joint estimation of electric-vehicle lithium-ion batteries.

LIU, D., WANG, S., FAN, Y., FERNANDEZ, C. and BLAABJERG, F.

2024

Journal of Energy Storage

A novel multi-factor fuzzy membership function - adaptive extended Kalman filter algorithm for the state of charge and energy joint estimation of electric-vehicle lithium-ion batteries

--Manuscript Draft--

Manuscript Number:	EST-D-23-05890
Article Type:	Research Paper
Keywords:	Multi-factor coupling model; Fuzzy membership function; State of charge; State of energy
Corresponding Author:	Shunli Wang, Prof.Dr. Southwest University of Science and Technology Mianyang, CHINA
First Author:	Donglei Liu
Order of Authors:	Donglei Liu Shunli Wang, Prof.Dr. Yongcun Fan Carlos Fernandez Frede Blaabjerg
Abstract:	<p>In view of the unmeasurable state parameters of electric-vehicle lithium-ion batteries, this paper investigates a novel multi-factor fuzzy membership function - adaptive extended Kalman filter (MFMF-AEKF) algorithm for the online joint estimation of the state of charge and energy. Strong nonlinear characteristics of model parameters are characterized by considering multiple processing factors of electrochemical and diffusion effects for lithium-ion batteries and constructing an optimized multifactor coupling model. In the proposed MFMF-AEKF method, multi-space-scale factors are introduced to realize the numerical analysis of the multi-factor coupled model parameters and state estimation under dynamic working conditions of electric-vehicle lithium-ion batteries. The proposed MFMF-AEKF algorithm estimates the state of charge (SOC) with the overall best mean absolute error (MAE), mean absolute percentage error (MAPE), root mean square error (RMSE), and maximum error (ME) values of 1.822%, 4.322%, 1.947%, and 2.954%, respectively, under challenging working conditions. And The MAE, MAPE, RMSE, and ME values for the state of energy (SOE) are 0.617%, 1.711%, 0.695%, and 1.011%, respectively. Both state estimation results are better than the traditional method. The proposed MFMF-AEKF algorithm has higher estimation accuracy which provides a feasible estimation algorithm for the joint SOC and SOE of lithium-ion batteries.</p>
Suggested Reviewers:	Yujie Wang wangyujie@ustc.edu.cn Yunlong Shang yshang@sdu.edu.cn

A novel multi-factor fuzzy membership function - adaptive extended Kalman filter algorithm for the state of charge and energy joint estimation of electric-vehicle lithium-ion batteries

Donglei Liu^a, Shunli Wang^{a,b*}, Yongcun Fan^a, Carlos Fernandez^c, Frede Blaabjerg^d

^aSchool of Information Engineering, Southwest University of Science and Technology, Mianyang 621010, China; ^bCollege of Electrical Engineering, Sichuan University, Chengdu 610065, China; ^cSchool of Pharmacy and Life Sciences, Robert Gordon University, Aberdeen AB10-7GJ, UK; ^dDepartment of Energy Technology, Aalborg University, Pontoppidanstraede 111 9220 Aalborg East, Denmark.

Abstract: In view of the unmeasurable state parameters of electric-vehicle lithium-ion batteries, this paper investigates a novel multi-factor fuzzy membership function - adaptive extended Kalman filter (MFMF-AEKF) algorithm for the online joint estimation of the state of charge and energy. Strong nonlinear characteristics of model parameters are characterized by considering multiple processing factors of electrochemical and diffusion effects for lithium-ion batteries and constructing an optimized multifactor coupling model. In the proposed MFMF-AEKF method, multi-space-scale factors are introduced to realize the numerical analysis of the multi-factor coupled model parameters and state estimation under dynamic working conditions of electric-vehicle lithium-ion batteries. The proposed MFMF-AEKF algorithm estimates the state of charge (SOC) with the overall best mean absolute error (MAE), mean absolute percentage error (MAPE), root mean square error (RMSE), and maximum error (ME) values of 1.822%, 4.322%, 1.947%, and 2.954%, respectively, under challenging working conditions. And The MAE, MAPE, RMSE, and ME values for the state of energy (SOE) are 0.617%, 1.711%, 0.695%, and 1.011%, respectively. Both state estimation results are better than the traditional method. The proposed MFMF-AEKF algorithm has higher estimation accuracy which provides a feasible estimation algorithm for the joint SOC and SOE of lithium-ion batteries.

Keywords: Muti-factor coupling model; Fuzzy membership function; State of charge; State of energy

*Corresponding author: Shunli Wang. E-mail address: wangshunli1985 @qq.com

1 Introduction

1.1 Literature review

Given the current global energy crisis, all nations are focused on investigating the sustainable development of new energy sources.^[1,2] New energy and energy storage systems have become an important part of new energy promotion and energy revolution^[3,4]. Due to their high energy density^[5], long cycle life, and low self-discharge rate^[6], lithium-ion batteries have emerged as the primary energy storage medium for new energy vehicles. Lithium-ion battery packs often occur in safety accidents during operation^[7,8], which is caused by the differences between battery cells and the increased inconsistency between the cells due to the complexity of the discharge working conditions^[9,10]. These potential risks greatly constrain the development of battery pack applications^[11]. In the current safety incidents of electric vehicle fires^[12], the main causes fall into two categories. One is caused by production or design defects of the battery or the circuit itself, and the other is caused by improper management during the use of the battery pack. Battery management system (BMS) research is crucial for battery applications^[13-15]. By ensuring a safe and reliable battery management system, potential safety incidents during battery usage can be effectively avoided, thus guaranteeing the secure application of power lithium-ion batteries^[16]. Accurately assessing the SOC and SOE, which are vital parameters at the core of the BMS, is of utmost significance^[17,18]. Both Hu et al^[19] and Wang et al^[20] proposed in their research on power lithium-ion batteries. They suggest that battery state estimation is crucial for BMS applications. The state parameter estimation in BMS still has the problem of low accuracy, which restricts the performance of power lithium-ion batteries as well as EVs in actual use, although power lithium-ion batteries have now achieved wide application in EVs^[21,22].

As the basis of core state estimation, equivalent circuit modeling (ECM) and parameter identification for power batteries are very important^[23,24]. ECM and parameter identification strategies are hot topics of interest for researchers^[25,26]. It has become a hot topic of interest for current scientific researchers, where equivalent modeling and filtering algorithms are used for more accurate state estimation^[27,28]. Zhang et al^[29] investigated the effect of load current on the parameters of the ECM, eliminating modeling errors and improving the accuracy of state estimation. Wang et al^[30] analyzed the specific factors for the variation of model parameters and constructed a nonlinear variation relationship between temperature and model parameters to enhance the precision of determining the state. Xu et al^[31] employed a simplified electrochemical

1
2 model to simulate the behavior of lithium-ion distribution within the battery under certain conditions and verified the validity
3
4 of the synergistic estimation of SOC and SOH. Liu et al^[32]. proposed an algorithm for estimating battery state that is based
5
6 on an autoregressive ECM to achieve joint multi-state online estimation.
7
8

9 In this paper, an ECM considering multi-factor coupling is constructed based on the study of the mechanism of key
10
11 coupled equivalent circuit parameters from the electrochemical intrinsic kinetics and diffusion effects of lithium-ion
12
13 batteries. A novel MFMF-AEKF algorithm is developed for application in the joint estimation of the SOC and SOE for
14
15 batteries. A multi-factor fuzzy membership function algorithm is formed by the analysis of electrochemical and physical
16
17 properties and the design of fuzzy reasoning, which can ensure the accurate acquisition at complex operating conditions on
18
19 the state parameters of the nonlinear system for lithium-ion batteries, thus supplying a vital assurance for the secure
20
21 functioning of the BMS.
22
23
24

25 26 **1.2 Idea and contribution**

27
28 The internal electrochemical polarization and physical diffusion processes inherent in lithium-ion batteries engender
29
30 coupled characteristics among the parameters of the ECM, reflecting the system's strong nonlinearity. In this research, the
31
32 online parameter identification and core state parameter estimation are realized by using the MFMF-AEKF algorithm for
33
34 the multiparameter coupling characteristic combined with the characteristic experimental results. The key accomplishments
35
36 of this paper can be summarized as follows.
37
38
39

40 (1) Aiming at the strongly coupled nonlinear characteristics characterized by the superior electrochemical intrinsic
41
42 kinetics and diffusion effects exhibited by the lithium-ion battery system, the characterization experiments that can be used
43
44 for parametric multi-factor fuzzy parameter identification are designed.
45
46

47 (2) A novel MFMF algorithm is designed to get the parameters of Multi-factor coupled ECM.
48
49

50 (3) Construction of an online joint estimation strategy for SOC and SOE of lithium-ion battery using the MFMF-AEKF
51
52 algorithm is presented, and the effectiveness of core state estimation is verified under two complex operating conditions,
53
54 which introduces a novel approach for estimating the core state of the power battery.
55
56

57 **1.3 Paper organization**

58
59 The remaining sections of this paper are structured as follows. In the second part, an ECM considering multi-factor
60
61 coupling is established, and a novel MFMF algorithm for parameter identification is designed and proposes a novel approach,
62
63
64
65

the MFMF-AEKF algorithm, to conduct an online simultaneous estimation of both SOC and SOE. In the third part, the characteristic experimental design is presented and the validity of the proposed algorithm for estimating the core state is verified under two complex experimental conditions. The fourth part offers a conclusion.

2 Mathematical analysis

2.1 Multi-factor coupling model

It is a necessary prerequisite for state estimation to construct an ECM that can accurately describe the electrochemically coupled nonlinear system of lithium-ion batteries. In the research, the non-linear electrochemical reactions and physical phenomena accompanying the working process are described based on the electrochemical and dynamic experimental features of batteries, using the discharge rate (C) and SOC as the research object.

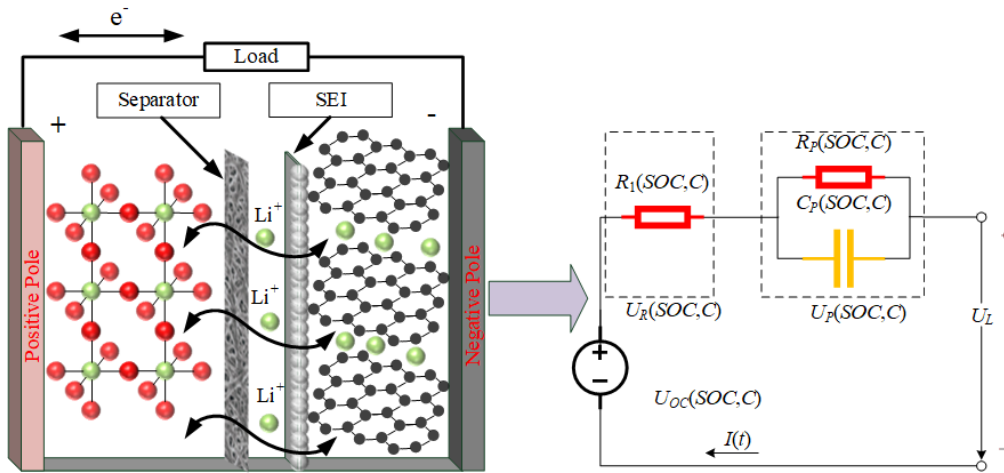


Figure 1 Multi-factor coupled ECM

The ECM of lithium-ion batteries considering multiple factors is realized by applying the analytic lithium-ion battery electrochemical coupling and discharge characteristics, and the constructed multi-factor coupled ECM is shown in Figure 1. The energy is stored and released by embedding and de-embedding Li^+ between two battery poles to realize the energy transfer process of batteries. The open circuit voltage exhibited externally by the lithium-ion battery when discharged to a certain SOC at a certain C is different, and this electrochemical characteristic is represented with a voltage source, as shown in Figure 1 for $U_{oc}(SOC, C)$. Also at a certain SOC different C will result in different resistance to the lithium-ion ions in the electrolyte as they pass through the separator as well as the SEI layer. The resistance experienced by the lithium-ion battery causes a voltage drop during discharge. The characteristics of this drop are the same as those of an ohmic resistor, as shown in Figure 1 for $R_1(SOC, C)$, which has a voltage of $U_R(SOC, C)$ across its terminals.

1
2 The speeds at which the positive and negative lithium ions get and lose electrons occur instantaneously, during the
3
4 operation of the battery. This leads to electrochemical polarization at the electrode. The diffusion process of Li^+ dissolved
5
6 in the electrolyte to the other electrode plate is relatively slow, and this slow process will produce a difference in lithium-
7
8 ion concentration between the two electrodes. The concentration difference polarization is caused by this physical diffusion
9
10 ion process. The electrochemical and concentration polarizations are manifested in the slow change of discharge voltage during
11
12 the discharge process. This slowly changing electrochemical characteristic is identical to that of a resistor-capacitor in
13
14 parallel, as shown in Figure 1 for $R_P(SOC, C)$ and $C_P(SOC, C)$, with the voltage across them as $U_P(SOC, C)$. $I(t)$ indicates
15
16 operating current, and in this paper, the positive direction of the current is considered to be during discharging. According
17
18 to the ECM considering the multi-factor coupling characteristics, the discharge voltage equation during the operation can
19
20 be obtained as shown in Equation (1).

$$21 \quad U_L = U_{OC}(SOC, C) - U_R(SOC, C) - U_P(SOC, C) \quad (1)$$

22
23 In Equation 1 U_L represents the discharge voltage shown in the battery's operation. It can be seen from Figure 1 that
24
25 the current flowing through $R_1(SOC, C)$ is equal to the current flowing through the parallel $R_P(SOC, C)$ and $C_P(SOC, C)$, i.e.,
26
27 the external discharge current $I(t)$, as shown in Equation (2).

$$28 \quad I(t) = C_P \frac{dU_P}{dt} + \frac{U_P}{R_P} \quad (2)$$

29
30 The equation for estimating the SOC and SOE is shown in Equation (3). In the equation $SOC(k+1)$ is the value of SOC
31
32 at moment $k+1$, $SOC(k)$ is the value of SOC at moment k , $I(k)$ is the magnitude of discharge current at moment k , η_1 denotes
33
34 charge/discharge efficiency in charge state, Q_N denotes rated capacity, $SOE(k+1)$ is the value of SOE at moment $k+1$, SOE
35
36 (k) is the value of SOE at moment k , η_2 denotes charge/discharge efficiency in energy state, E_N denotes rated capacity, and
37
38 $U_L(k)$ is the value of discharge voltage at moment k .

$$39 \quad \begin{cases} SOC(k+1) = SOC(k) - I(k) \frac{\eta_1 \Delta t}{Q_N} \\ SOE(k+1) = SOE(k) - I(k) \frac{\eta_2 U_L(k) \Delta t}{E_N} \end{cases} \quad (3)$$

40
41
42
43
44
45
46
47
48
49
50
51
52
53
54
55
56
57
58
59
60
61
62
63
64
65

$$\begin{cases}
\begin{bmatrix} SOC(k+1) \\ SOE(k+1) \\ U_p(k+1) \end{bmatrix} = \begin{bmatrix} 1 & 0 & 0 \\ 0 & 1 & 0 \\ 0 & 0 & e^{\frac{-\Delta t}{R_p C_p}} \end{bmatrix} + I(k) \begin{bmatrix} -\frac{\eta_1 \Delta t}{Q_N} \\ -\frac{\eta_2 U_L(k) \Delta t}{E_N} \\ R_p (1 - e^{\frac{-\Delta t}{R_p C_p}}) \end{bmatrix} + w \\
U_L(k+1) = U_{OC}(k+1) - R_1(k+1) + \begin{bmatrix} 0 \\ -1 \end{bmatrix}^T \begin{bmatrix} SOE(k+1) \\ U_p(k+1) \end{bmatrix} + v
\end{cases} \quad (4)$$

The state space equations and observation equations for the joint estimation of SOC and SOE are shown in Equation (4).

In Equation (4), $U_p(k+1)$ is the value of the polarization voltage at moment $k+1$. $U_L(k+1)$ is the value of the discharge voltage at moment $k+1$. $R_1(k+1)$ is the value of $R_1(\text{SOC}, C)$ at moment $k+1$. w is the process noise matrix. v is the observation noise matrix. The noise w and v are considered Gaussian white noise in the calculation process.

2.2 MFMF Parameter identification algorithm

The multifactor coupled ECM is analyzed, and factors such as the electrochemical and diffusion processes of lithium-ion batteries lead to changes in the parameters of the ECM. The SOC and C are selected as inputs for the model parameter identification based on the analysis of the ECM, and the parameters of the ECM are taken as outputs. The parameter identification strategy based on fuzzy logic rules consists of four parts: fuzzifier, knowledge base, fuzzy operation, and defuzzifier. The fuzzifier is a mapping that completes the transformation of input variables into fuzzy single values; the knowledge base consists of two parts, namely the database and the rule base.; the fuzzy operation is the center of the fuzzy rule-based system; the defuzzifier is a mapping that completes the transformation from fuzzy output to unfuzzy output. In this research, the identification of the multi-factor coupled ECM constructed requires the use of a multi-input multi-output fuzzy algorithm. Multi-input multi-output fuzzy algorithms are formed by combining several multi-input single-output fuzzy algorithms. Therefore, only one multi-input single-output fuzzy algorithms case is given below. This parameter identification method uses the Mamdani fuzzy system. Figure 2 is the MFMF Parameter identification system.

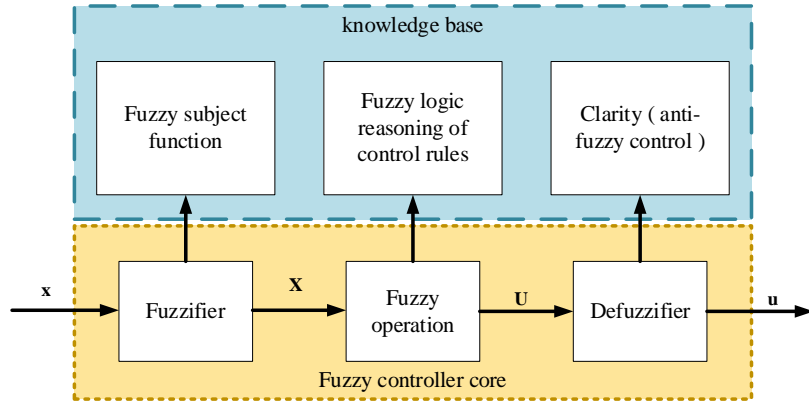


Figure 2 The MFMF Parameter identification system

The fuzzy parameter recognition controller contains a fuzzifier, a fuzzy inference machine, a defuzzifier, and a fuzzy rule base, as shown in Figure 2. The fuzzifier can apply a fuzzy membership function to map the exact input x to a fuzzy subset X . The fuzzy inference machine implements a fuzzy estimate based on a fuzzy rule base to obtain the total output U of fuzzy inference. The defuzzifier can obtain the exact output value u by defuzzification. In this research, the triangular membership function is used for all fuzzy affiliation functions, as shown in Equation (5).

$$f(x, c, d, e) = \begin{cases} 0 & x \leq c \\ \frac{x-c}{d-c} & c \leq x \leq d \\ \frac{e-x}{e-d} & d \leq x \leq e \\ 0 & x \geq e \end{cases} \quad (5)$$

$$R1: \text{IF } x_1 \text{ is } A_1^l \text{ AND } x_2 \text{ is } A_2^l \text{ AND...AND } x_n \text{ is } A_n^l \text{ THEN } u \text{ is } B^l \quad (6)$$

$$u = \frac{\int_s u \mu_B(u) du}{\int_s \mu_B(u) du} \quad (7)$$

In Equation (5), parameters c and d determine the two base angles of the triangle, and parameter e determines the top angle of the triangle. In this paper, the IF-THEN control rule is used to realize the fuzzy application calculation. The fuzzy rule applied is shown in Equation (6). In Equation (6), A_i^l ($i=1, 2, \dots, n$) is the input fuzzy set of the input variable x . B^l is the output fuzzy set of output variable y . In this paper, we use the center of gravity method to implement the defuzzification, as shown in Equation (7). The membership function of u , denoted as μ_B , determines the degree to which u belongs to a fuzzy set, where u represents the output value of the fuzzy algorithm.

2.3 MFMF-AEKF joint online estimation algorithm

The purpose of ECM and parameter identification is to accomplish the estimation of the unmeasurable parameters inside the battery. However, SOC and SOE are such unmeasurable states. In this research, online parameters identification and joint estimation for internal states under the effect of multifactor coupling are realized, using the MFMF-AEKF algorithm.

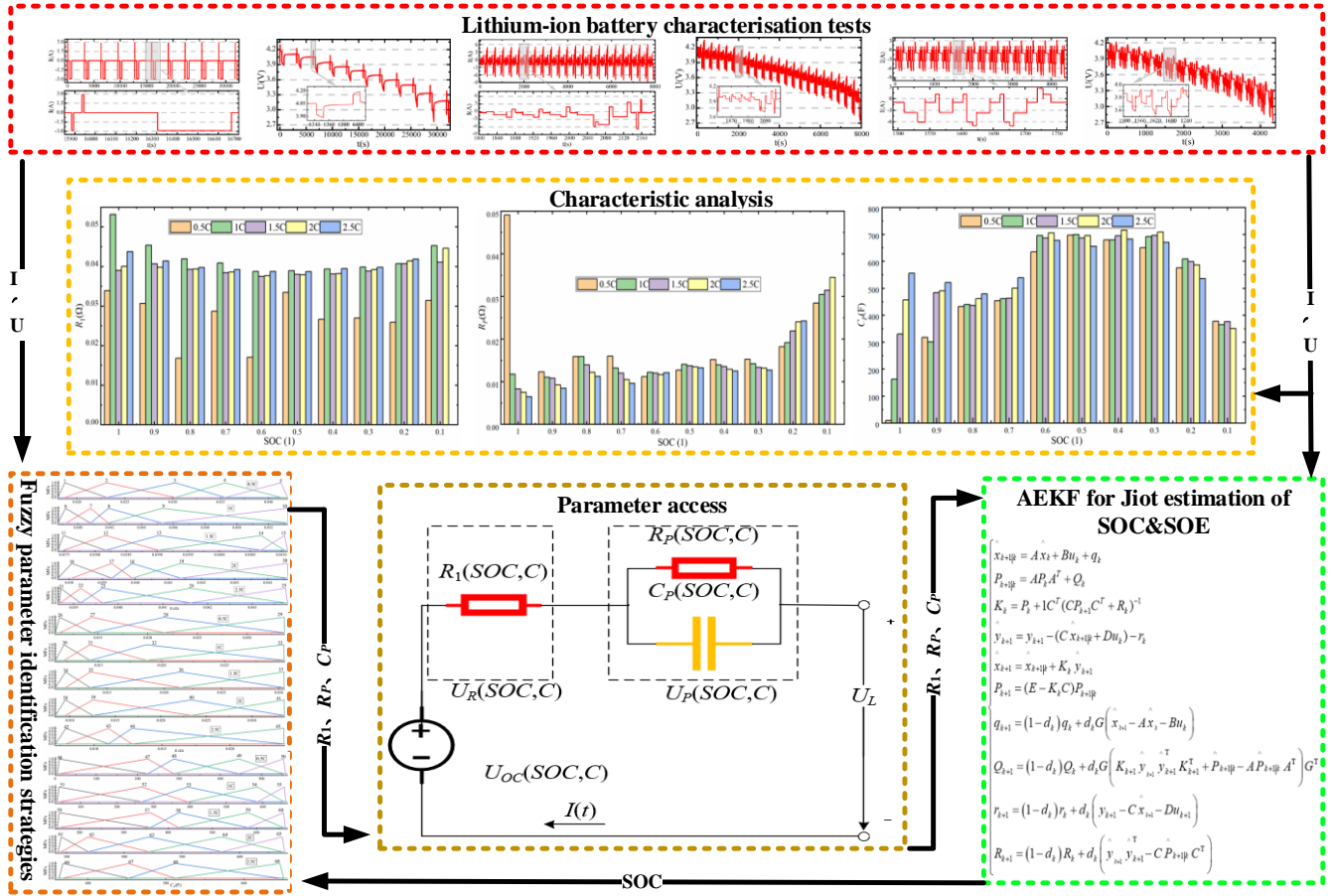


Figure 3 MFMF-AEKF joint online estimation algorithm flow chart

Firstly, the charge/discharge characteristics analysis is completed based on the lithium-ion battery characteristics experiments. Second, the full-parameter online identification of the multi-factor coupled ECM under the effect of multi-factor coupling is realized. Finally, the online SOC and SOE estimation is achieved combine the AEKF. Figure 3 shows the flow chart of the MFMF-AEKF joint online estimation algorithm.

In Figure 3, the working characteristics of the lithium-ion battery and the ECM parameter distribution law under the

1
2 coupling effect of multiple factors are obtained through characteristic experimental analysis. The real-time parameters
3
4 identification of the multi-factor coupled model is realized by using fuzzy membership functions based on the working
5
6 characteristic analysis. The inputs to the membership function are the SOC and the C. The C can be obtained by
7
8 measurement. The SOC is estimated by the AEKF. Using such a closed-loop estimator, iterative estimation of the battery
9
10 SOC and SOE is realized. Equation (8) shows the operator equation for the AEKF algorithm.

$$\begin{cases}
 \hat{x}_{k+1|k} = A \hat{x}_k + B u_k + q_k \\
 P_{k+1|k} = A P_k A^T + Q_k \\
 K_k = P_{k+1} C^T (C P_{k+1} C^T + R_k)^{-1} \\
 \hat{y}_{k+1} = y_{k+1} - (C \hat{x}_{k+1|k} + D u_k) - r_k \\
 \hat{x}_{k+1} = \hat{x}_{k+1|k} + K_k \hat{y}_{k+1} \\
 P_{k+1} = (E - K_k C) P_{k+1|k} \\
 q_{k+1} = (1 - d_k) q_k + d_k G \left(\hat{x}_{k+1} - A \hat{x}_k - B u_k \right) \\
 Q_{k+1} = (1 - d_k) Q_k + d_k G \left(K_{k+1} \hat{y}_{k+1} \hat{y}_{k+1}^T K_{k+1}^T + \hat{P}_{k+1|k} - A \hat{P}_{k+1|k} A^T \right) G^T \\
 r_{k+1} = (1 - d_k) r_k + d_k \left(y_{k+1} - C \hat{x}_{k+1} - D u_{k+1} \right) \\
 R_{k+1} = (1 - d_k) R_k + d_k \left(\hat{y}_{k+1} \hat{y}_{k+1}^T - C \hat{P}_{k+1|k} C^T \right)
 \end{cases} \quad (8)$$

40 In Equation (8), $\hat{x}_{k+1|k}$ is the state variable at moment $k+1$ predicted at moment k . A means the state transfer matrix.

41
42
43 \hat{x}_k means the state variable at moment k . B means the control matrix. u_k means the control variable of the control matrix.

44
45
46 q_k , Q_k , r_k and R_k are noise variables. P_k means the error covariance. K_k means the Kalman gain. C means the

47
48
49 system measurement matrix. y_{k+1} means the new interests. D means the driving prediction matrix. E means the unit

50
51
52 matrix. d_k means the weighting factor. G means noise-driven.

53 3 Experiments and discussions

54 3.1 Experimental platform

55
56
57
58
59
60 A brand of 18650 power cell commonly used in EVs is chosen for the experiment. The battery is rated at 3080mAh

1
2 capacity and 3.6V voltage, an operating range of 2.75V-4.2V, a maximum discharge multiplier of 3C, and a normal
3
4 operating temperature of -10~40°C. Figure 4 shows the multi-factor coupled experimental analysis platform for lithium-ion
5
6 batteries.

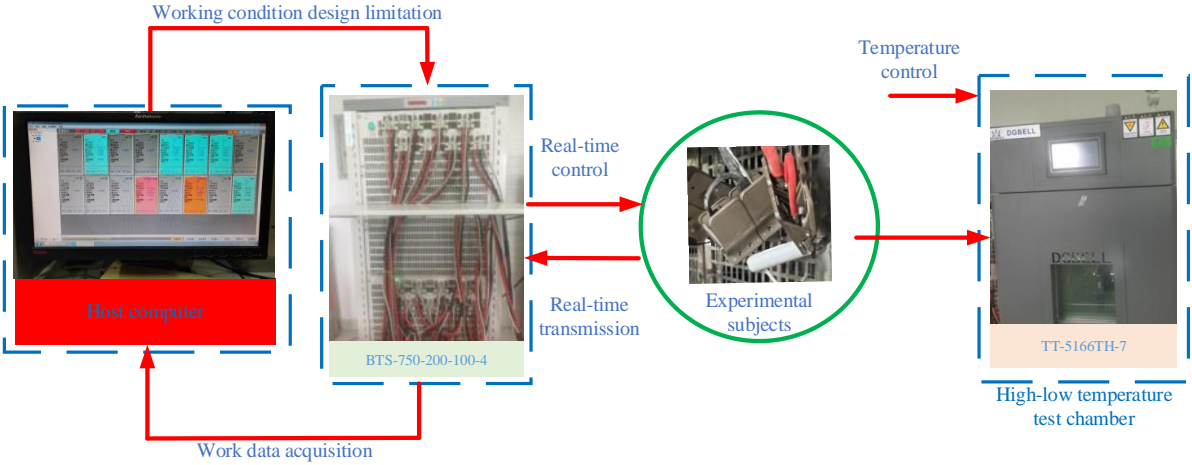


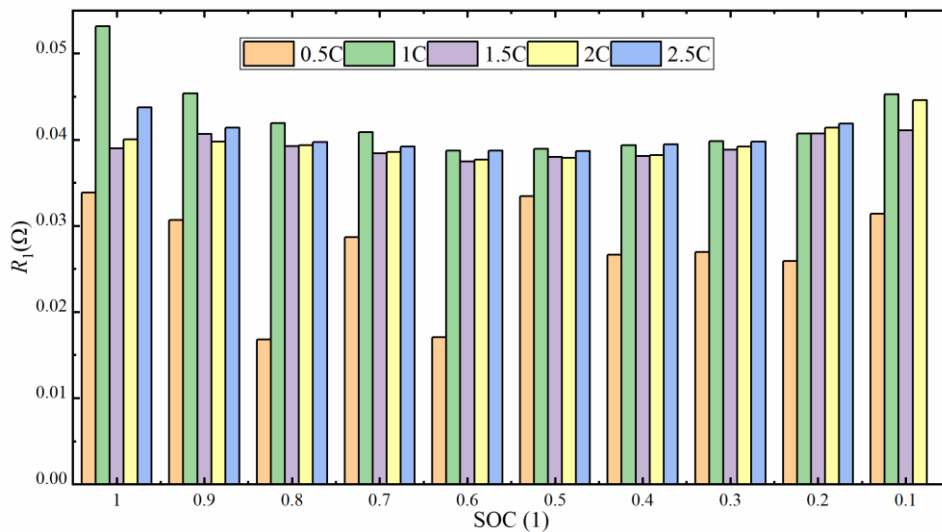
Figure 4 The multi-factor coupled experimental analysis platform

The experimental equipment is utilized to perform three tests on lithium-ion batteries, including the charge/discharge characteristics test, dynamic stress test (DST), and Beijing bus dynamic stress test (BBDST) separately. The purpose of these tests is to assess the performance and behavior of the batteries under different conditions and stresses, including charging, discharging, and dynamic operation. By conducting these tests, important data can be obtained and insight into the electrochemical performance, capacity, efficiency and safety of the battery can be gained. Based on the data analysis, the algorithm construction and estimation effect verification of MFMF-AEKF in the multi-space scale can be completed.

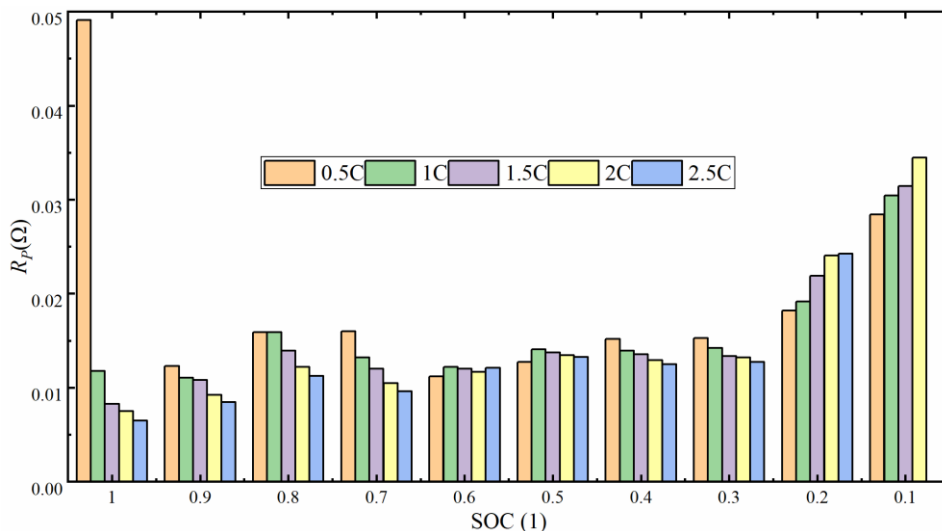
3.2 MFMF online parameter identification analysis results

The parameters of the multi-factor coupled ECM are influenced by multiple factors, and the discharge process exhibits a strong nonlinear trend. The polarization effect is formed by the migration of electrons and diffusion of ions during the electrochemical reaction in lithium-ion batteries. The hindering effect of the diaphragm and the SEI layer, etc. during ion diffusion at a certain discharge intensity, i.e., a certain discharge multiplicity, leads to the generation of ohmic polarization internal resistance. The SOC is related to the ion concentration and thus affects the diffusion effect. The diffusion rate of ions in lithium-ion batteries corresponds to the discharge intensity, i.e., the discharge rate multiplier. To obtain the discharge characteristics of multi-factor coupled ECM parameters at different SOC and C, experiments related to the discharge characteristics of lithium-ion batteries are designed. Thus, an MFMF recognition inference machine fuzzy rule base is

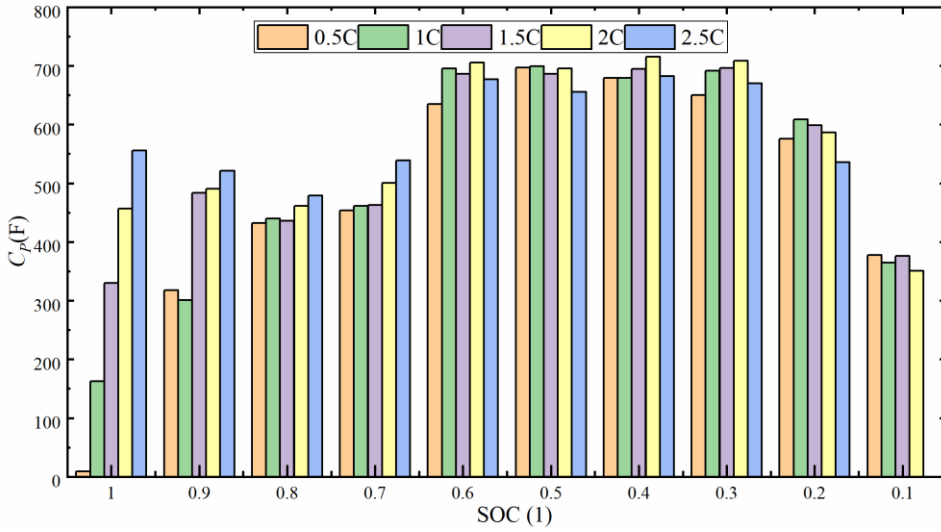
developed to realize the fuzzy online recognition of multi-factor coupled ECM parameters. The analytical results of the experiment are shown in Figure 5.



(a) Internal ohmic polarization resistance histogram



(b) Polarization resistance histogram



(c) Polarization Capacitance Histogram

Figure 5 Multi-factor coupled ECM discharge characterization analysis

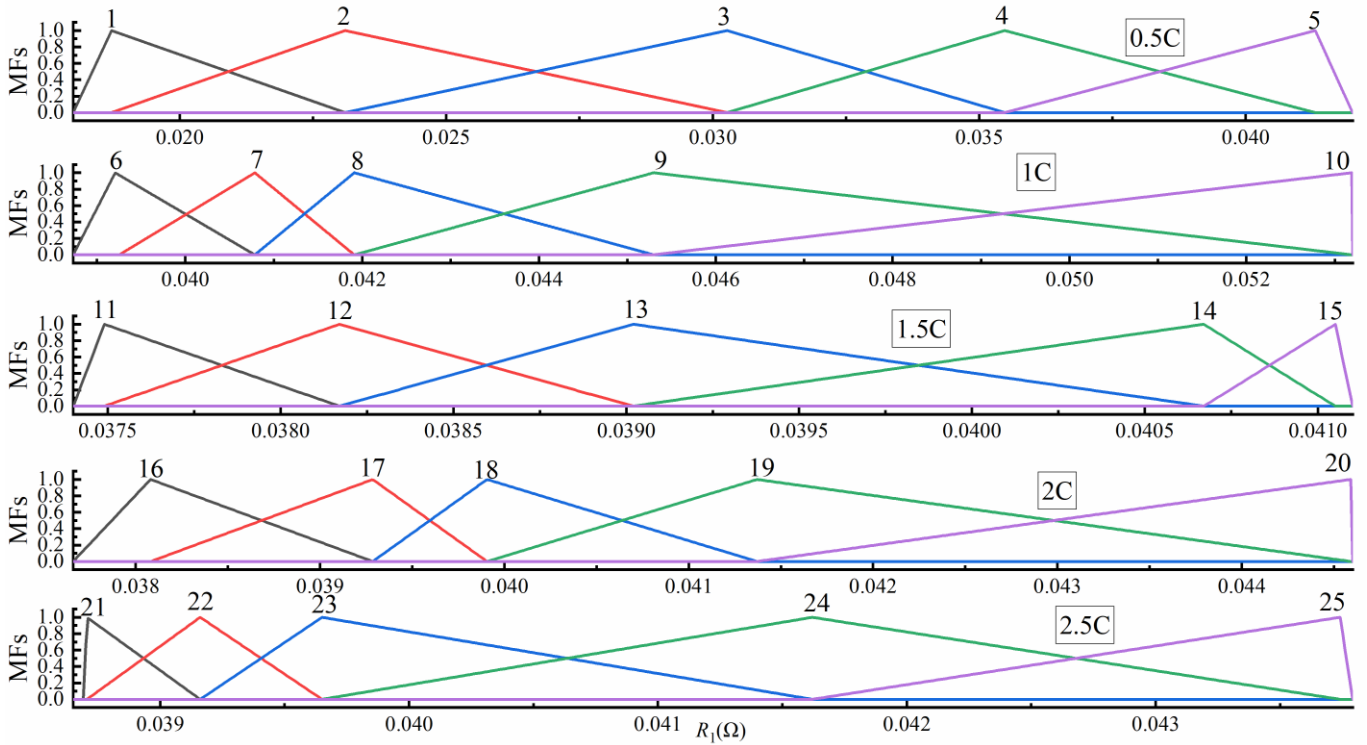
As can be seen in Figure 5, at the same SOC, the model parameters are different, and this difference is caused by the difference in electrochemical reactions and diffusion effects due to the C. The resistance to ions passing through the diaphragm and the SEI layer is relatively low under low C conditions. The internal resistance of ohmic polarization increases when the discharge rate increases. At a relatively high SOC, the electrochemical and densely polarized resistances are relatively high at low C. The polarization capacitance, however, is the opposite of the polarization resistance.

Table 1 Fuzzy rules under different C and SOC

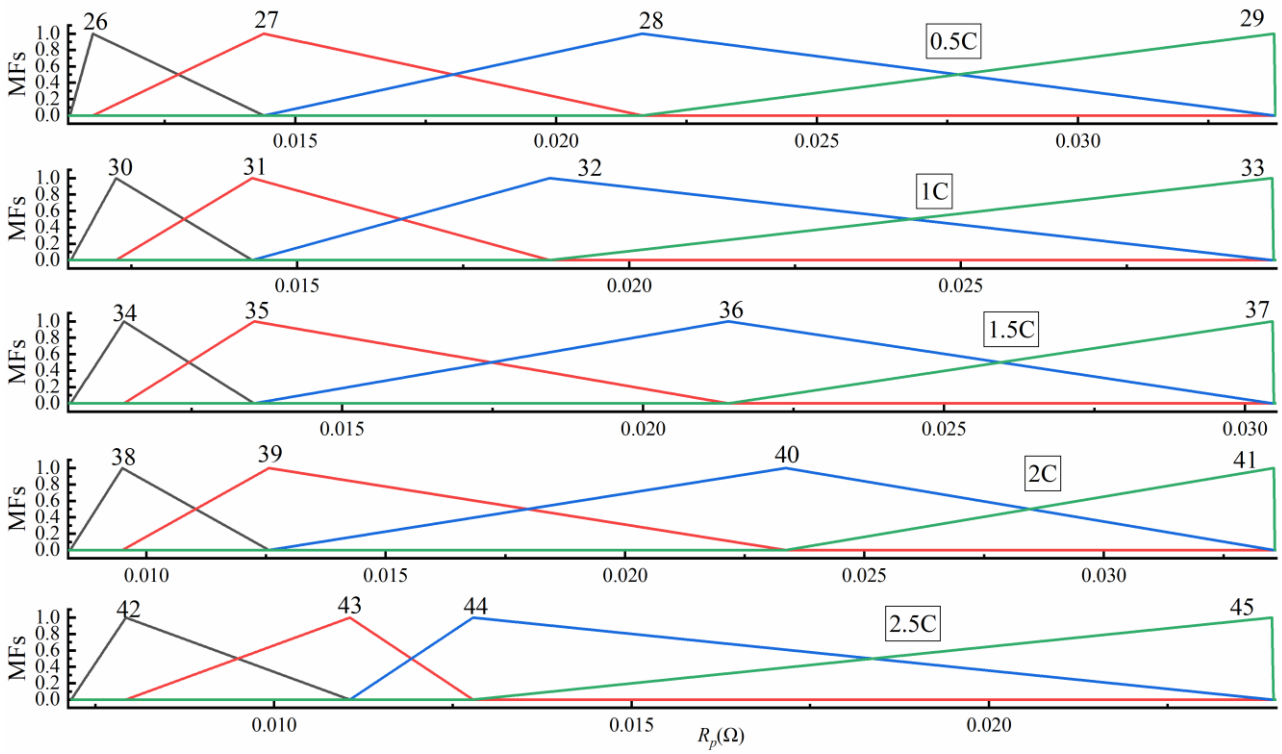
Parameter	$R_1(SOC,C)$					$R_p(SOC,C)$					$C_p(SOC,C)$				
C \ SOC	0.5	1	1.5	2	2.5	0.5	1	1.5	2	2.5	0.5	1	1.5	2	2.5
1	3	10	13	18	25	29	32	34	38	42	46	51	56	61	66
0.9	3	9	14	18	24	27	30	34	38	42	47	52	58	63	67
0.8	2	8	13	17	23	27	31	35	39	43	47	53	58	63	67
0.7	2	7	12	16	22	27	30	34	38	43	47	53	58	63	68
0.6	1	6	11	16	21	26	30	34	39	43	47	55	60	65	69
0.5	2	6	12	16	21	26	31	35	39	44	48	55	60	65	69

1																
2	0.4	4	6	12	16	23	26	31	35	39	44	50	55	60	65	69
3																
4	0.3	2	6	13	17	23	26	31	35	39	44	48	55	60	65	69
5																
6	0.2	3	7	14	19	24	26	32	36	40	45	49	54	59	64	68
7																
8	0.1	5	9	15	20		28	33	37	41		49	53	57	62	
9																

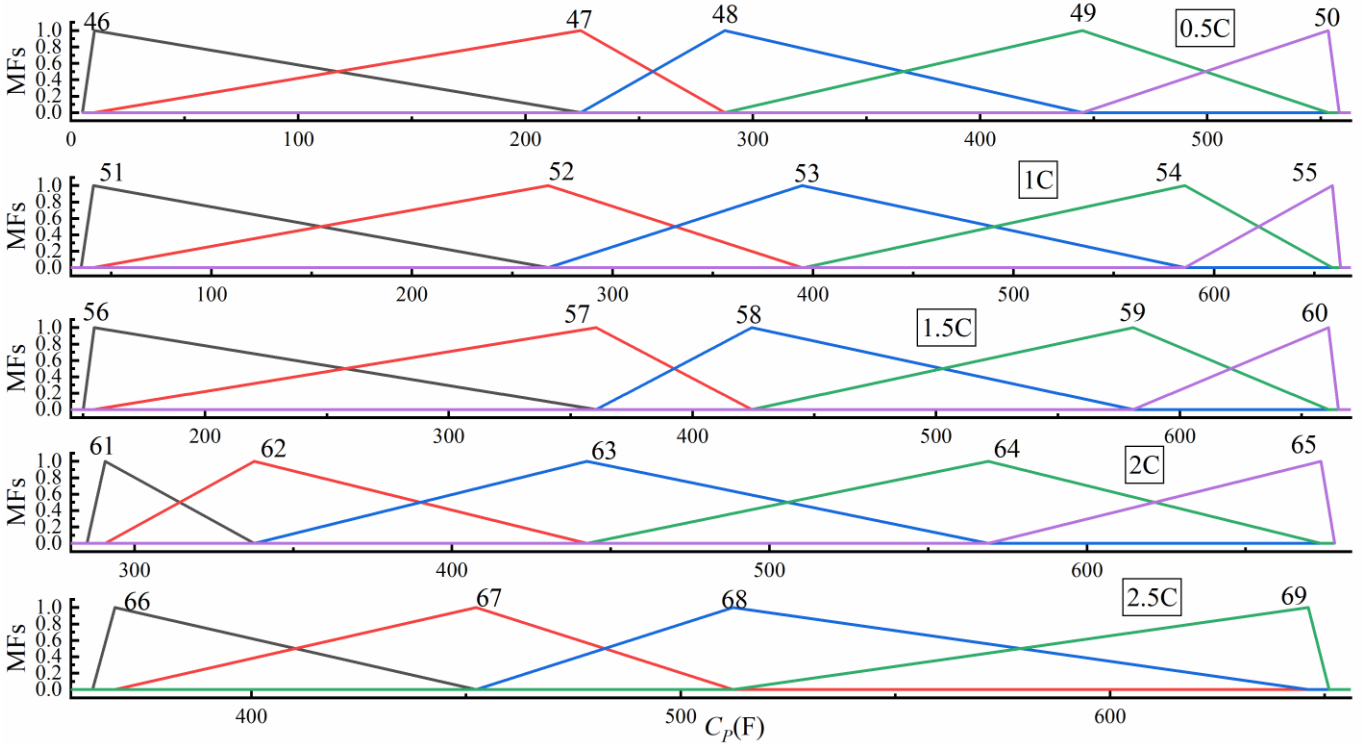
Fuzzy rule table for the identification of the parameters of the lithium-ion multi-factor coupled ECM under different SOC and C, based on the results obtained from the experimental analysis of the discharge characteristics. Table 1 develops the model parameter rules for different C at 10 SOC. According to the fuzzy rules, the triangular membership function is chosen and the fuzzy membership function is shown in Figure 6.



(a) Internal ohmic polarization resistance membership function



(b) Polarization resistance membership function



(c) Polarization capacitance membership function

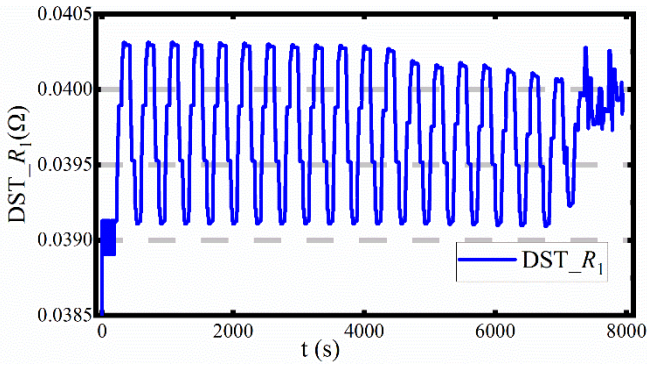
Figure 6 MFMF online parameter identification function

In Figure 6, five fuzzy rules are applied to identify the internal ohmic polarization resistance parameters at different

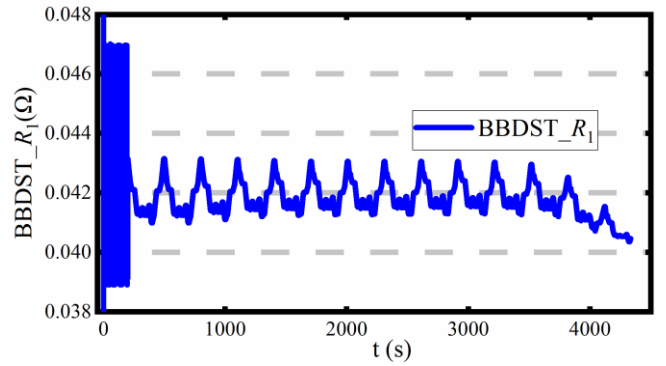
SOCs for each C. There are 25 fuzzy membership functions used for internal ohmic polarization resistance to achieve online identification under the effect of multi-factor coupling. Online parameter identification of the polarization resistance is achieved using four fuzzy rules for each C. For polarization resistance, 20 fuzzy membership functions are applied to achieve online parameter identification under the effect of multi-factor coupling. For the polarization capacitance, 24 fuzzy membership functions are used to achieve online parameter identification under the effect of multi-factor coupling.

3.3 Validation of estimation results

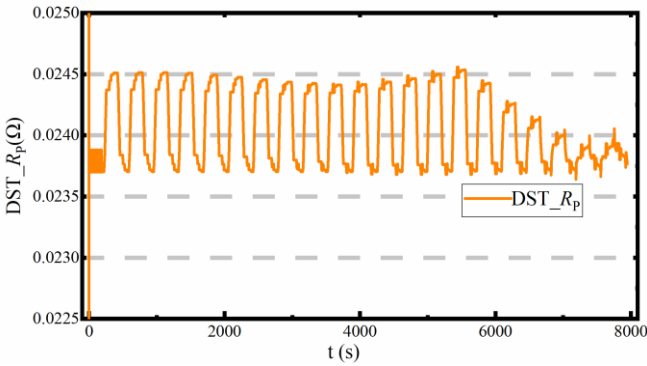
The estimation of both SOC and SOE states is achieved separately under the experimental conditions of DST and BBDST, respectively. The performance of the lithium-ion battery varies between the two operating conditions, i.e., the C is not the same. The results of the lithium-ion battery multi-factor coupled ECM parameters under the two operating conditions are shown in Figure 7.



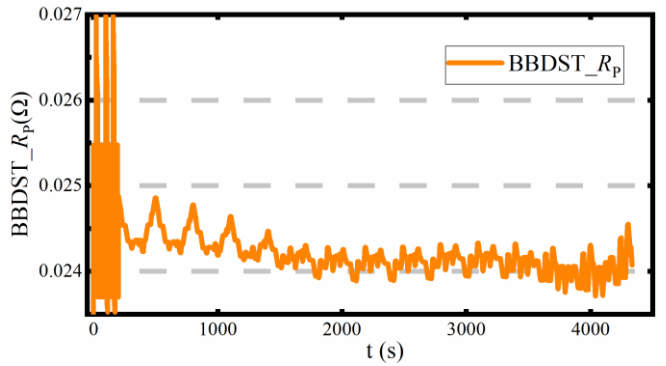
(a) Internal ohmic polarization resistance in DST operation



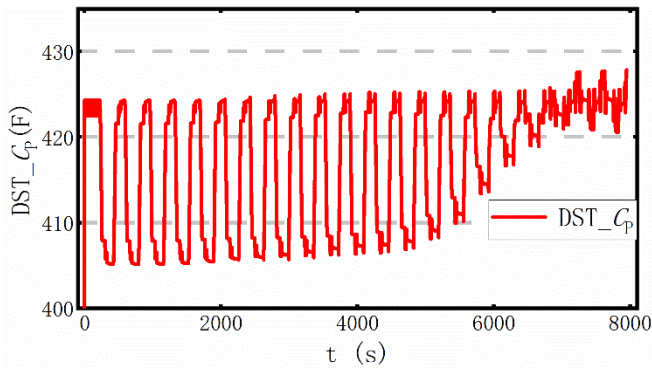
(b) Internal ohmic polarization resistance in BBDST operation



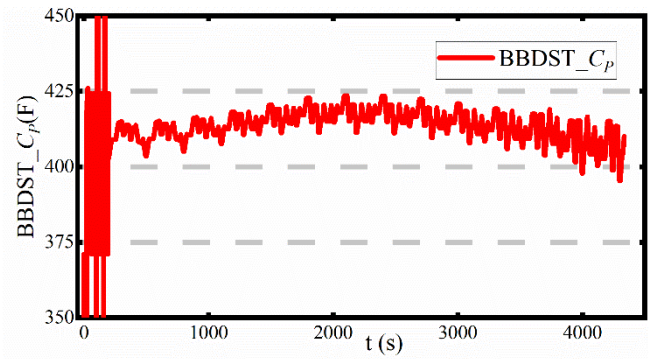
(c) Polarization resistance in DST operation



(d) Polarization resistance in BBDST operation



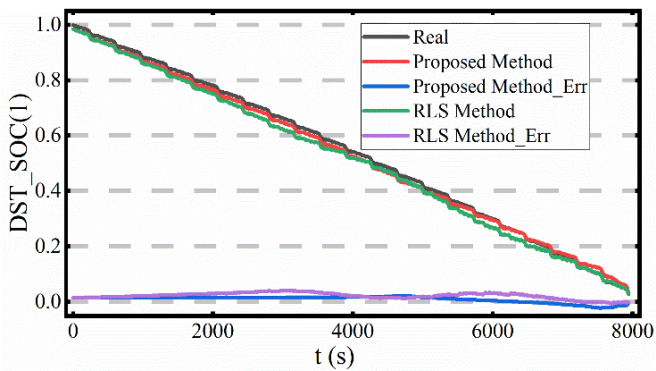
(e) Polarization capacitance in DST operation



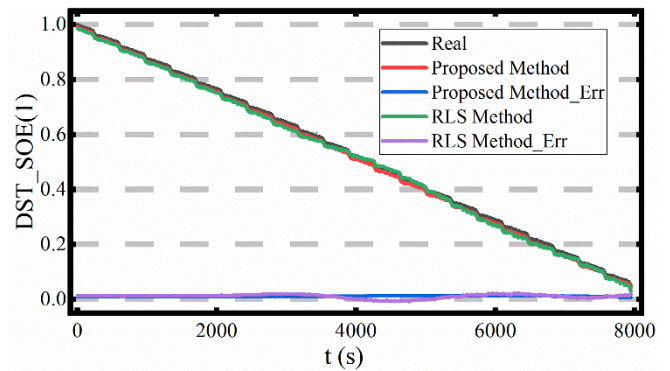
(f) Polarization capacitance in BBDST operation

Figure 7. Results of online parameter identification using MFMF

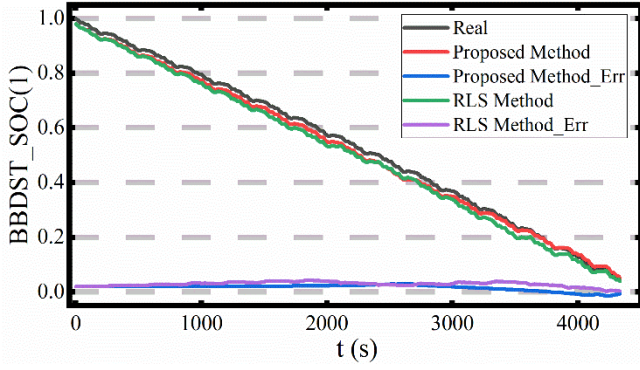
In Figure 7, the values of the same variable of the multi-factor coupled model are different for different operating conditions. The result follows the change of C and SOC. The reason for these differences is the difference in electrochemical and diffusion processes within the lithium-ion battery under different operating conditions. Such changes occur within a certain range without parameter divergence due to the limitations of the fuzzy algorithm. The parameters show a tendency to change periodically, which is due to the cyclic working condition setting. At the same time, this trend of change is also in accordance with the law of change summarized by the characteristic experiment. Two methods are applied in two experimental conditions, the proposed joint method and the RLS method. The results of SOC and SOE estimates calculated by the two methods are shown in Figure 8.



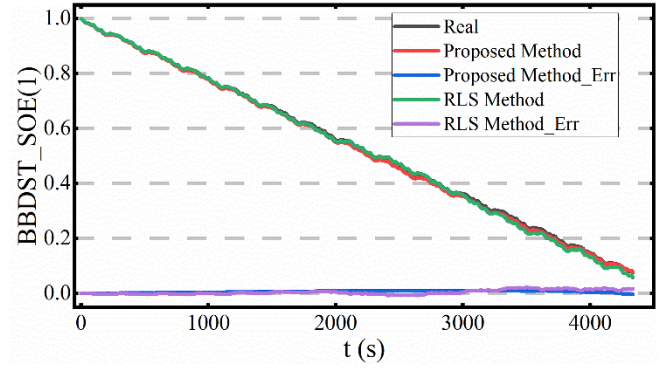
(a) SOC results under DST conditions



(b) SOE results under DST conditions



(c) SOC results under BBDST conditions



(d) SOE results under BBDST conditions

Figure 8 Online joint estimation results of MFMF-AEKF under two operation conditions

The joint estimation of the SOC and SOE is realized in both operating conditions, respectively. The results of state estimation under DST experimental conditions are shown in Figure. 8(a) and Figure. 8(b). It can be seen that both algorithms achieve good estimation results for joint state estimation, and the estimation results fluctuate above and below the true value. The estimation results obtained by using the proposed method under the BBDST experimental conditions are shown in Figure. 8(c) and Figure. 8(d). Similarly, the estimation results fluctuate around the true value. Table 2 displays the evaluation of the proposed algorithm's performance compared to the RLS algorithm for estimating SOC

Table 2 SOC performance evaluation table under different operating conditions

Method & Evaluation	DST_RLS	DST_Proposed	Improve	BBDST_RLS	BBDST_Proposed	Improve
MAE (%)	2.269	1.377	39.312	2.863	1.822	36.360
MAPE (%)	4.836	4.219	12.759	7.053	4.322	38.721
RMSE (%)	2.497	1.468	41.209	2.980	1.947	34.664
ME (%)	4.138	2.280	44.909	4.294	2.954	31.211

MAE, MAPE, RMSE, and ME are used to confirm the accuracy and robustness of the estimation approach. The MAE, MAPE, RMSE, and ME of SOC estimation by RLS estimation method under DST experimental conditions are 2.269%, 4.836%, 2.497%, and 4.138%, respectively. Meanwhile, the MAE, MAPE, RMSE, and ME of the proposed method to estimate SOC are 1.377%, 4.219%, 1.468%, and 2.280%, respectively. The convergence of the estimated effect is better than the paper ^[33]. MAE, MAPE, RMSE, and ME improved by 39.312%, 12.759%, 41.209%, and 44.909%, respectively. Likewise, the MAE, MAPE, RMSE, and ME of the RLS estimation method for estimating SOC under the BBDST experimental condition are 2.863%, 7.053%, 2.980%, and 4.294%, respectively. The MAE, MAPE, RMSE, and ME of the proposed method for estimating SOC are 1.822%, 4.322%, 1.947%, and 2.954%, respectively. MAE, MAPE,

RMSE, and ME improved by 36.360%, 38.712%, 34.664%, and 31.211%, respectively. The aforementioned outcomes validate that the suggested estimation approach demonstrates higher accuracy and robustness. The performance evaluation table of the proposed algorithm and the RLS algorithm for estimating SOE is shown in Table 3.

Table 3 SOE performance evaluation table under different operating conditions

Method & Evaluation	DST_RLS	DST_Proposed	Improve	BBDST_RLS	BBDST_Proposed	Improve
MAE (%)	1.197	1.090	8.939	0.655	0.617	5.802
MAPE (%)	3.584	3.265	8.900	2.932	1.711	41.644
RMSE (%)	1.314	1.096	16.590	0.907	0.695	23.374
ME (%)	2.419	1.229	49.167	2.115	1.011	52.181

The MAE, MAPE, RMSE, and ME of SOE estimated by the RLS estimation method under the DST experimental condition are 1.197%, 3.584%, 1.314%, and 2.419%, respectively. Meanwhile, the MAE, MAPE, RMSE, and ME of the proposed method to estimate SOE are 1.090%, 3.265%, 1.096%, and 1.229%, respectively. The convergence of the estimated effect is better than the paper^[34]. MAE, MAPE, RMSE, and ME improved by 8.939%, 8.900%, 16.590%, and 49.167%, respectively. The MAE, MAPE, RMSE, and ME of SOE estimation by the RLS estimation method under BBDST experimental conditions are 0.655%, 2.932%, 0.907%, and 2.115%, respectively. The proposed method has better MAE, MAPE, RMSE, and ME of 0.617%, 1.711%, 0.695%, and 1.011% for estimating SOE, respectively. The convergence of the estimated effect is better than the paper^[35]. MAE, MAPE, RMSE, and ME improved by 5.802%, 41.644%, 23.374%, and 52.181%, respectively. The joint estimation of SOC and SOE was verified under two experimental conditions. Both achieved good estimation accuracy and robustness.

4 Conclusions

In this paper, the multi-factor strong nonlinear coupling characteristics of lithium-ion batteries are analyzed, and a multi-factor coupled ECM is constructed. A novel MFMF online parameter identification algorithm for ECMs is proposed for application to simultaneously estimate both SOC and SOE for lithium-ion batteries. The MFMF-AEKF algorithm is formed by a multi-factor fuzzy logic inference system based on the characteristic analysis, which can ensure the accurate obtaining of the state parameters under complex operating conditions of the lithium-ion battery nonlinear system, thus providing a significant assurance for the secure functioning of the BMS. When used for SOC estimation, the MAE, MAPE, RMSE, and ME are improved by 39.312%, 12.759%, 41.209%, and 44.909%, respectively, compared with the traditional

1
2 algorithm in the DST operation. Compared to the traditional algorithm, the BBDST experimental condition resulted in a
3
4 36.360% improvement in MAE, 38.712% improvement in MAPE, 34.664% improvement in RMSE, and 31.211%
5
6 improvement in ME. When used for SOE estimation, the MAE, MAPE, RMSE, and ME are improved by 8.939%, 8.900%,
7
8 16.590%, and 49.167%, respectively, compared with the traditional algorithm in the DST experimental condition.
9
10 Compared to the traditional algorithm, the BBDST experimental condition results in an improvement of 5.802% for MAE,
11
12 41.644% for MAPE, 23.374% for RMSE, and 52.181% for ME. The experimental verification results demonstrate that the
13
14 proposed MFMF-AEKF algorithm has higher estimation accuracy which provides a feasible estimation algorithm for the
15
16 joint SOC and SOE of lithium-ion batteries.
17
18
19

20 21 **Acknowledgments**

22
23 The work is supported by the National Natural Science Foundation of China (No. 62173281, 61801407), Natural
24
25 Science Foundation of Southwest University of Science and Technology (No. 17zx7110, 18zx7145), Robot Technology
26
27 Used for Special Environment Key Laboratory Fund of Sichuan Province (No. 18kftk03), and Robert Gordon University.

28 29 **References**

- 30
31 [1] Cui Z H, Dai J Y, Sun J R, et al. Hybrid Methods Using Neural Network and Kalman Filter for the State of Charge
32
33 Estimation of Lithium-Ion Battery[J]. *Mathematical Problems in Engineering*, 2022, 2022: 1-13.
- 34
35 [2] Lipu M S H, Hannan M A, Hussain A, et al. Data-driven state of charge estimation of lithium-ion batteries:
36
37 Algorithms, implementation factors, limitations and future trends[J]. *Journal of Cleaner Production*, 2020, 277: 1-29.
- 38
39 [3] Zhang T, Guo N Y, Sun X X, et al. A Systematic Framework for State of Charge, State of Health and State of
40
41 Power Co-Estimation of Lithium-Ion Battery in Electric Vehicles[J]. *Sustainability*, 2021, 13(9): 1-19.
- 42
43 [4] Zhu C, Shang Y L, Lu F, et al. Core Temperature Estimation for Self-Heating Automotive Lithium-Ion Batteries
44
45 in Cold Climates[J]. *Ieee Transactions on Industrial Informatics*, 2020, 16(5): 3366-3375.
- 46
47 [5] Zhou Z K, Duan D, Kang Y Z, et al. An efficient screening method for retired lithium -ion batteries based on
48
49 support vector machine[J]. *Journal of Cleaner Production*, 2020, 267: 1-12.
- 50
51 [6] Zhao G Q, Liu Y, Liu G, et al. State-of-charge and state-of-health estimation for lithium-ion battery using the
52
53 direct wave signals of guided wave[J]. *Journal of Energy Storage*, 2021, 39: 1-12.
- 54
55 [7] Mohammadi F. Lithium-ion battery State-of-Charge estimation based on an improved Coulomb-Counting
56
57 algorithm and uncertainty evaluation[J]. *Journal of Energy Storage*, 2022, 48: 1-10.
- 58
59 [8] Kang Y Z, Yang X C, Zhou Z K, et al. A comparative study of fault diagnostic methods for lithium-ion batteries
60
61 based on a standardized fault feature comparison method[J]. *Journal of Cleaner Production*, 2021, 278: 1-13.
- 62
63 [9] Nawaz M, Ahmed J, Abbas G. Energy-efficient battery management system for healthcare devices[J]. *Journal of*
64
65 *Energy Storage*, 2022, 51: 1-11.
- 66
67 [10] Sun Q, Lv H Y, Wang S S, et al. Optimized State of Charge Estimation of Lithium-Ion Battery in SMES/Battery
68
69 Hybrid Energy Storage System for Electric Vehicles[J]. *Ieee Transactions on Applied Superconductivity*, 2021, 31(8): 1-

6.

[11] Ge M F, Liu Y B, Jiang X X, et al. A review on state of health estimations and remaining useful life prognostics of lithium-ion batteries[J]. *Measurement*, 2021, 174: 1-27.

[12] Zhang J N, Yang X G, Sun F C, et al. An online heat generation estimation method for lithium-ion batteries using dual-temperature measurements[J]. *Applied Energy*, 2020, 272: 1-12.

[13] Ji S Y, Sun Y, Chen Z X, et al. A Multi-Scale Time Method for the State of Charge and Parameter Estimation of Lithium-Ion Batteries Using MIUKF-EKF[J]. *Frontiers in Energy Research*, 2022, 10: 1-13.

[14] Wang S L, Takyi-Aninakwa P, Yu C M, et al. Improved Compound Correction-Electrical Equivalent Circuit Modeling and Double Transform-Unscented Kalman Filtering for the High-Accuracy Closed-Circuit voltage and State-of-Charge Co-Estimation of Whole-Life-Cycle Lithium-Ion batteries[J]. *Energy Technology*, 2022, 10(12): 1-13.

[15] Li A G, Wang W Z, West A C, et al. Health and performance diagnostics in Li-ion batteries with pulse-injection-aided machine learning[J]. *Applied Energy*, 2022, 315: 1-9.

[16] Wang Y J, Tian J Q, Sun Z D, et al. A comprehensive review of battery modeling and state estimation approaches for advanced battery management systems[J]. *Renewable & Sustainable Energy Reviews*, 2020, 131: 1-18.

[17] Zhang M Y, Wang S L, Yang X, et al. A Novel Square Root Adaptive Unscented Kalman Filter Combined with Variable Forgetting Factor Recursive Least Square Method for Accurate State-of-charge Estimation of Lithium-Ion Batteries[J]. *International Journal of Electrochemical Science*, 2022, 17(9): 1-15.

[18] Fan T E, Liu S M, Tang X, et al. Simultaneously estimating two battery states by combining a long short-term memory network with an adaptive unscented Kalman filter[J]. *Journal of Energy Storage*, 2022, 50: 1-12.

[19] Hu X, Feng F, Liu K, et al. State estimation for advanced battery management: Key challenges and future trends[J]. *Renewable and Sustainable Energy Reviews*, 2019, 114: 109334.

[20] Wang Y, Tian J, Sun Z, et al. A comprehensive review of battery modeling and state estimation approaches for advanced battery management systems[J]. *Renewable and Sustainable Energy Reviews*, 2020, 131: 110015.

[21] Xiao R X, Hu Y W, Jia X G, et al. A novel estimation of state of charge for the lithium-ion battery in electric vehicle without open circuit voltage experiment[J]. *Energy*, 2022, 243: 1-14.

[22] Tian J P, Xiong R, Shen W X, et al. Deep neural network battery charging curve prediction using 30 points collected in 10 min[J]. *Joule*, 2021, 5(6): 1521-1534.

[23] Shu X, Li G, Shen J W, et al. A uniform estimation framework for state of health of lithium-ion batteries considering feature extraction and parameters optimization[J]. *Energy*, 2020, 204: 1-10.

[24] Dong G Z, Xu Y, Wei Z B. A Hierarchical Approach for Finite-Time H-infinity State-of-Charge Observer and Probabilistic Lifetime Prediction of Lithium-Ion Batteries[J]. *Ieee Transactions on Energy Conversion*, 2022, 37(1): 718-728.

[25] Chen M Y, Han F L, Shi L, et al. Sliding Mode Observer for State-of-Charge Estimation Using Hysteresis-Based Li-Ion Battery Model[J]. *Energies*, 2022, 15(7): 1-14.

[26] An F L, Jiang J C, Zhang W G, et al. State of Energy Estimation for Lithium-Ion Battery Pack via Prediction in Electric Vehicle Applications[J]. *Ieee Transactions on Vehicular Technology*, 2022, 71(1): 184-195.

[27] Liu Y W, Shi Q, Wei Y J, et al. State of charge estimation by square root cubature particle filter approach with fractional order model of lithium-ion battery[J]. *Science China-Technological Sciences*, 2022, 65(8): 1760-1771.

- 1
2 [28] Xing L K, Ling L Y, Gong B, et al. State-of-charge estimation for Lithium-Ion batteries using Kalman filters
3 based on fractional-order models[J]. Connection Science, 2022, 34(1): 162-184.
4
5 [29] Zhang W J, Wang L Y, Wang L F, et al. Joint State-of-Charge and State-of-Available-Power Estimation Based
6 on the Online Parameter Identification of Lithium-Ion Battery Model[J]. Ieee Transactions on Industrial Electronics, 2022,
7 69(4): 3677-3688.
8
9 [30] Wang Q, Gao T, Li X C. SOC Estimation of Lithium-Ion Battery Based on Equivalent Circuit Model with
10 Variable Parameters[J]. Energies, 2022, 15(16): 1-15.
11
12 [31] Xu Z C, Wang J, Lund P D, et al. Co-estimating the state of charge and health of lithium batteries through
13 combining a minimalist electrochemical model and an equivalent circuit model[J]. Energy, 2022, 240: 1-14.
14
15 [32] Liu F, Shao C, Su W X, et al. Online joint estimator of key states for battery based on a new equivalent circuit
16 model[J]. Journal of Energy Storage, 2022, 52: 1-15.
17
18 [33] Shi N, Chen Z W, Niu M, et al. State-of-charge estimation for the lithium-ion battery based on adaptive
19 extended Kalman filter using improved parameter identification[J]. Journal of Energy Storage, 2022, 45: 1-13.
20
21 [34] Dong G Z, Chen Z H, Wei J W, et al. An online model-based method for state of energy estimation of lithium-
22 ion batteries using dual filters[J]. Journal of Power Sources, 2016, 301: 277-286.
23
24 [35] Yang X, Wang S L, Xu W H, et al. A novel fuzzy adaptive cubature Kalman filtering method for the state of
25 charge and state of energy co-estimation of lithium-ion batteries[J]. Electrochimica Acta, 2022, 415: 1-13.
26
27
28
29
30
31
32
33
34
35
36
37
38
39
40
41
42
43
44
45
46
47
48
49
50
51
52
53
54
55
56
57
58
59
60
61
62
63
64
65

The authors declare that they have no known competing financial interests or personal relationships that could have appeared to influence the work reported in this paper.

- Strong nonlinear characteristics of model parameters are characterized by considering multiple processing factors of electrochemical and diffusion effects for lithium-ion batteries and constructing an optimized multifactor coupling model.
- In the proposed MFMF-AEKF method, multi-space-scale factors are introduced to realize the numerical analysis of the multi-factor coupled model parameters and state estimation under dynamic working conditions of electric-vehicle lithium-ion batteries.
- The effectiveness of core state estimation is verified under two complex operating conditions, which provides a new strategy for core state estimation of power lithium-ion batteries.